Influence of water on the intrinsic characteristics of cellulose dissolved in an ionic liquid

Koide, Mitsuharu; Urakawa, Hiroshi; Kajiwara, Kanji; Rosenau, Thomas; Wataoka, Isao

Published in:
Cellulose

DOI:
10.1007/s10570-020-03323-2

Published: 01/09/2020

Document Version
Accepted author manuscript

Document License
Publisher rights policy

Influence of water on the intrinsic characteristics of cellulose dissolved in an ionic liquid

Mitsuharu Koide,[1] Hiroshi Urakawa,[2] Kanji Kajiwara,[3] Thomas Rosenau[1,4] Isao Wataoka[2,*]

[1] Division of Chemistry of Renewables, Department of Chemistry, University of Natural Resources and Life Sciences, Vienna (BOKU), Muthgasse 18, A-1190, Vienna, Austria

[2] Department of Biobased Materials Science, Faculty of Fiber Science and Engineering, Kyoto Institute of Technology, Matsugasaki, Sakyo-ku, Kyoto City, Kyoto 6068585, Japan

[3] Faculty of Textile Science and Technology, Shinshu University, 3-15-1 Tokida, Ueda City, Nagano 3868567, Japan

[4]Johan Gadolin Process Chemistry Centre, Åbo Akademi University, Porthansgatan 3, Åbo/Turku FI-20500, Finland

Corresponding author: Isao Wataoka, wataoka@kit.ac.jp

Abstract

The local structure of cellulose, dissolved in the frequently used ionic liquid EMIm-OAc, is modelled by a coaxial double layer cylinder. The cylinder´s core consists of a cellulose chain while the sheath is formed by a solvent layer with lower electron density than the bulk solvent. We studied 2% cellulose solutions in EMIm-OAc and their behavior upon addition of increasing amounts of water. At this cellulose concentration, 15 wt% of water induced the precipitation of cellulose. Water molecules did not form an independent phase, but were bound to EMIm-OAc in the cellulose/water/EMIm-OAc solution. The conformational of a cellulose chain changes by adding water into the solution, and the square of the apparent cross-sectional radius of gyration of the cellulose chain becomes zero to negative. This phenomenon is explained by the formation of a solvation shell with lower electron density than the bulk solvent around the cellulose chain.

Keywords

cellulose; cellulose solution; ionic liquid; small-angle X-ray scattering; coaxial double layer cylinder model; solvation model

Introduction

Cellulose is not soluble in ordinary organic solvents and requires special solvents to form solutions of independent, monomolecularly dispersed chains (Henniges et al. 2011). Certain metal complexes, organic compounds or salt solutions are used to dissolve cellulose for practical applications, such as cuen (copper-ethylenediamine) for viscosity measurements (Ahn et al. 2019), *N*-methylmorpholine-*N*-oxide monohydrate for cellulose fiber production (Rosenau et al. 1999) and *N,N*-dimethylacetamide/LiCl for gel permeation chromatography (Potthast et al. 2015). Salts that maintain a liquid state at room temperature instead of forming solid crystals are known as room-temperature ionic liquids (ILs). ILs have been known for some time as solvents of cellulose at room temperature (Swatloski et al. 2002). Although the mechanism of cellulose dissolution process is still not sufficiently well understood, a wide variety of ILs is available in the meantime for dissolution of cellulose and as reaction media (Heinze et al. 2005; Barthel and Heinze 2006; Fukaya et al. 2008). There have been theoretical and experimental studies on the process of cellulose dissolution in ILs, including the analysis by NMR (Moulthrop et al. 2005; Yongs et al. 2011), viscosity (Gericke et al. 2009), electro-magnetic wave scattering (Chen et al. 2011), molecular dynamics (Lynden-Bell et al. 2007; Liu et al. 2010; Rabideau et al. 2013; Zhao et al. 2013; Uto et al. 2018) and analysis of chemical side reactions and degradation processes (Rosenau, et al. 2005, Ebner et al. 2008, Liebner et al. 2010). According to earlier publications (Koide et al. 2019), a small amount of water – as low as 1 wt% – in ILs causes a serious problem in dissolving cellulose due to the competitive formation of hydrogen bonding between ionic liquids, water and cellulose (Swatloski et al. 2002). The influence of water upon precipitation of cellulose from solution in 1-butyl-3-methylimidazolium chloride (BMIm-Cl) was quantitatively evaluated by turbidimetric measurements (Mazza et al. 2008). The experimental cellulose dissolution limit and precipitation solubility limit were not the same, as seen for the example of EMIm-OAc (Hedlund 2015). In general, such solubility and precipitation studies confirmed a good solution power of BMIm-Cl and EMIm-OAc for cellulose, with turbidity seeming to increase consistently with higher cellulose concentration up to 6 wt% at 363.15 K. This increase of turbidity may indicate a formation of small aggregates of cellulose with sizes of less than 860 nm. The negative effect of water on dissolution was also touched in this study: the binary solvent system of BMIm-Cl and water is able to dissolve cellulose (1 wt%) at 368.15K if the water content stays lower than 17 wt%. Cellulose precipitated when the water content exceeded this limit. 1-Ethyl-3-methylimidazolium acetate (EMIm-OAc) dissolves cellulose at low concentrations (< 5 wt%) when the water content is below 15 wt% (Le et al. 2014). We have

chosen this solvent for our study because it is most widely used in cellulose science – it is easily available and cheap – and because there are no heavier atoms, such as Cl or P, which could interfere with the X-ray scattering. Since there had already been many studies on this solvent, the data situation was also better than for other liquids. The solubility of cellulose in EMIm-OAc was found to depend on concentration, the degree of polymerization (DP) and the water amount contained in EMIm-OAc (Olsson et al. 2014; Le et al. 2014; Parviainen et al. 2014; Hedlund et al. 2015). In general, cellulose solubility in EMIM-OAc and ionic liquids of the dialkylimidazolium type is governed by a rather complex interplay between cellulose concentration and water concentration, with the effect of the anti-solvent water becoming more pronounced with increasing cellulose concentration. When adding water, the solution remains transparent, the conformation of the cellulose chains will be affected, which eventually collapse with increasing non-solvent content. Since a cellulose chain is relatively rigid and its parts, conceivable as chain links, are approximately modelled by cylinders, the chain collapse of a cellulose chain proceeds differently from the usual chain collapse of a fully flexible polymer chain. In the preceding paper (Koide et al. 2019), we have analyzed the intrinsic properties of cellulose dissolved in ILs in terms of a coaxial double layer cylinder model. This simple rigid body model represents the local shape of a cellulose chain surrounded by solvents. Cellulose was found to be dissolved molecularly without aggregation in the ILs employed. The sheath (the outer layer) of a coaxial double cylinder consists of solvent molecules, which prevent cellulose chains from forming hydrogen bonds, in particular intermolecular ones. In this follow-up account, we employed small-angle X-ray scattering (SAXS) to observe the local structure of a cellulose chain during the process of adding water (non-solvent) to a solution of cellulose in EMIm-OAc, until cellulose precipitation commenced. The results are analyzed in terms of the previously applied coaxial double layer cylinder model.

Materials and Methods

Cellulose samples. Microcrystalline cellulose (MCC) with a degree of polymerization of DP = 170 (Avicel PH101, Lot no. BCBB5909) was purchased from Sigma–Aldrich. MCC was dried for six hours in a vacuum oven at 373 K before use. The ionic liquid EMIm-OAc (Lot no. STBC922V) with a purity of 95%, was purchased from Sigma–Aldrich. The IL was dried under vacuum for two hours at 353 K before use.

Preparation of cellulose/IL solutions. The sample solutions were prepared by weighing cellulose directly into the sample bottle and adding the solvent to adjust the intended concentrations of the solutions. To ensure complete dissolution, the solution was heated for four

hours at 353 K using a dry bath incubator while the temperature was continuously monitored. The sample bottles were sealed in order to avoid the moisture absorption from the ambient atmosphere and stored before the SAXS measurements. The solutions remained visibly transparent and showed no sign of discoloration due to side reactions or opacity due to cellulose precipitation throughout. The cellulose started to precipitate visibly from the 2.0 wt% solution when the water content exceeded 15 wt%.

The solvent used, EMIm-OAc, has a strong affinity to water and naturally absorbs moisture from the atmosphere naturally to increase its water content. In 80% relative humidity at room temperature, dry EMIm-OAc IL (water content <0.1%) absorbs 3.2 wt% water over 24 h.

Determination of water contents in the solution samples. The amounts of water in the EMIm-OAc/water binary solvent and in the ternary system of a cellulose/EMIm-OAc/water solution were quantitatively analyzed with a Karl Fischer Moisture Titrator (MKC-210, Kyoto Electronics Manufacturing Co., LTD, Japan). The reagents for the Karl-Fischer method were purchased from Nacalai Tesque, Japan. The original solvent (EMIm-OAc) contained 0.1-0.6 wt% water at the time of purchase. The water content in the cellulose/EMIm-OAc solutions was checked for each solution before the SAXS measurement.

Synchrotron X-ray scattering experiments. SAXS measurements were performed at the beamline BL6A (Shimizu et al. 2013) of Photon Factory (PF) in KEK (Tsukuba, Japan). An incident X-ray from synchrotron radiation was monochromatized to 0.150 nm. The X-ray scattering was detected by a two-dimensional semiconductor detector (PILATUS3 1M). The exact camera length was calibrated by using the diffraction peaks of silver behenate. The scattered X-ray irradiation was accumulated over a total measuring time of 3 min, this way preventing damage of the cellulose specimens by the X-ray impact.

The cellulose solutions were injected into flat stainless-steel cells provided with quartz windows, mounted onto the cell holder with the temperature being kept constant at 298 K. The scattered intensities were corrected with regard to the variation of the incident X-ray flux by observing the beam with forward and backward monitors, i.e. ionizing chambers placed in front and back of the sample holder. The excess scattering intensities were evaluated by subtracting the scattering intensities of solvent from those of cellulose solutions.

Results and Discussion

Small-angle X-ray scattering. The SAXS profiles from the cellulose solution (2 wt%) containing water in three different concentrations are shown in Figure 1 in terms of the Kratky

plots. According to equation (1) the scattering vectors q is defined in terms of the scattering angle as (Kajiwara and Wataoka 2016):

$$q = \frac{4\pi}{\lambda}\sin\theta \quad (1)$$

with 2θ being the scattering angle specified by the vectors of the scattered and incident X-ray directions, and λ being the wave length. The scattering profiles suggest that these solutions can be considered dilute because of the straight lines in the small q region. The cellulose chains are individualized and become less flexible in the presence of water; the profile at 15 % water exhibits a typical scattering profile of a thin rod without any cross-section. The scattering curves overlap at smaller scattering angles, indicating that the cellulose molecular shape as a whole would hardly change by the addition of water molecules. When q exceeds 2 nm^{-1}, the SAXS profiles from the cellulose solutions become different, changing with the water content. Since the scattering profile in this high q range reflects the local structures of molecules, this change in the profiles indicates the different mode of solvation of a cellulose chain and/or a local conformational change. The apparent thinning of cross-section could be caused by the contrast between solute and solvent due to the change of electron density in both phases.

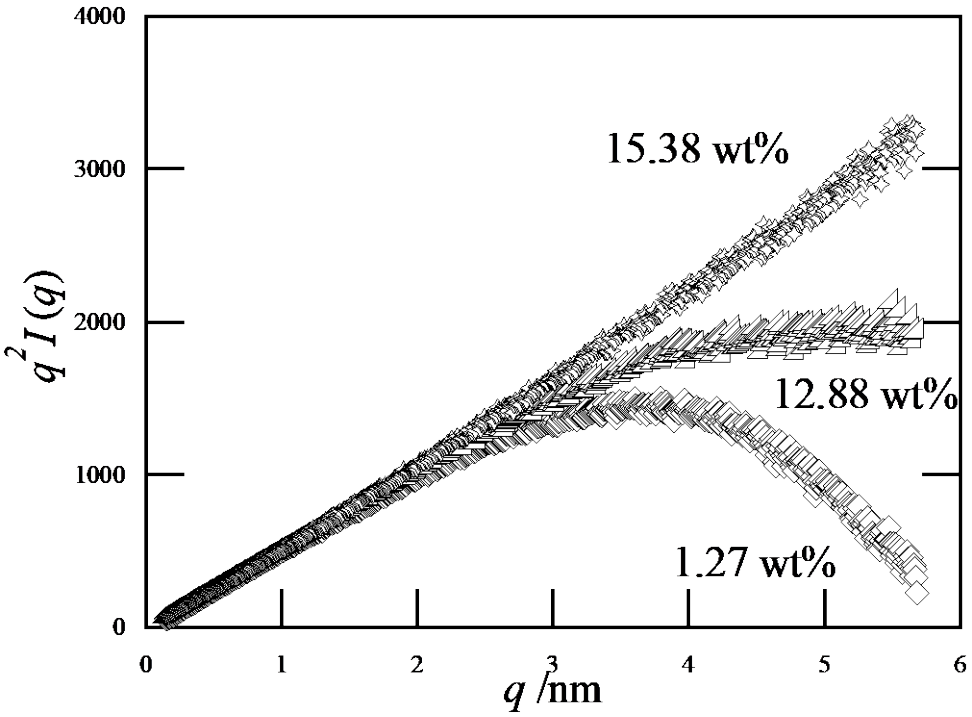

Figure 1. Cellulose in EMIm-OAc solution (2 wt%). Kratky plot as a function of the scattering vector q for three different water concentrations: 1.27 wt%, 12.88 wt%, and 15.38 wt%.

Chen et al. (2011) suggested that cellulose adopts a rigid conformation in EMIm-OAc, so that the dimension of the cross-section could be evaluated from SAXS profiles by a conventional Guinier approximation. A cellulose chain assumes a rigid rod-like shape at least locally over the range observed by SAXS. The scattering intensity from such a rigid molecule is approximately represented by the scattering from a cylinder constituted of two components (see eq. 2), that is, in a radial and axial direction (Kajiwara and Wataoka 2016):

$$P_{cylinder}(q) \approx \frac{\pi}{2Hq} \cdot P_c(q) \quad (2)$$

where $P_c(q)$ and 2H denote the scattering function from the cross-section and the height of the cylinder, respectively. The factor 1/q is characteristic of a rigid rod-like particle, and eq. (2) is valid only when the condition $Hq < 1$ is met. The scattering function from the cross-section of a rigid rod-like molecule is given in equation (3) by the Guinier approximation in terms of the cross-sectional radius of gyration Rc (Kajiwara and Wataoka 2016):

$$P(q) = \exp\left(-\frac{q^2 R_c^2}{2}\right) \quad (3)$$

Equations (2) and (3) imply that the initial negative slope of $\ln\{qI(q)\}$ plotted against q^2 (the Guinier plot for cross-section) in Figure 2 yields a quantity equivalent to $R_c^2/2$. However, the observed SAXS profiles change with increasing concentration of water in solution, yielding an apparently smaller cross-sectional radius of gyration with increasing water contents when the Guinier approximation for cross-section according to eq. (3) is applied. The apparent cross-sectional radius of gyration takes an unrealistic negative value when the water content reaches 15 wt%, which is the limit to dissolve cellulose in the binary EMIm-OAc/water solvent. Thus, the conventional analysis based on the assumption of a single boundary between solute and solvent fails in the present system of cellulose/EMIm-OAc/water at higher water contents.

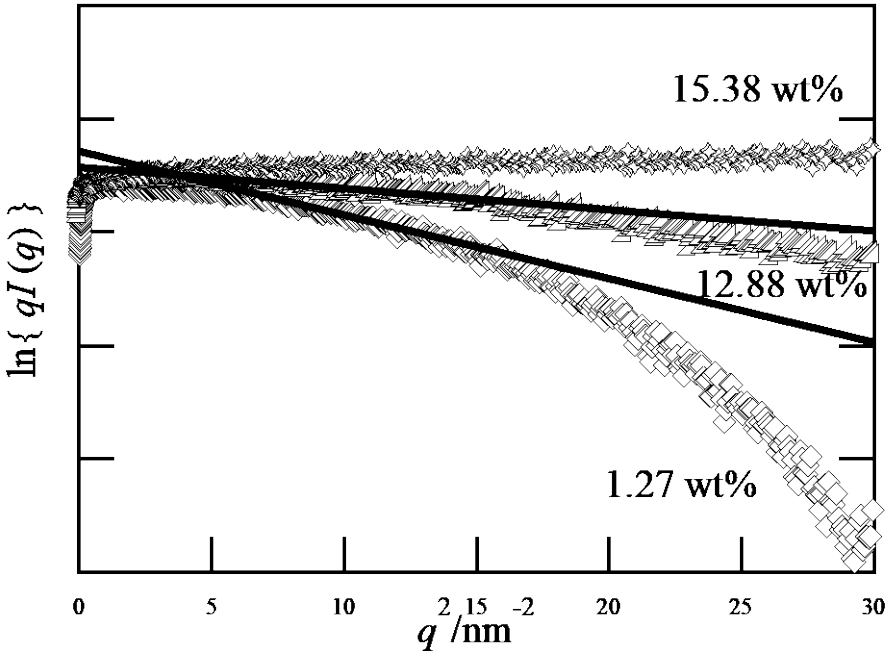

Figure 2. Cross-sectional Guinier plots for EMIm-OAc/Water/Avicel cellulose. Solid lines show the Guinier approximations.

Coaxial double-layer cylinder model. Following the results of the preceding paper (Koide et al. 2019), we adopt a coaxial double-layer cylinder model to the cellulose/EMIm-OAc/water system and elucidate the effect of water on the SAXS profiles and subsequent cross-sectional analyses. Livsey (1987) has shown that the slope of cross-sectional Guinier plots from a coaxial double-layer cylinder model (a sheath/core model) could have a positive value under certain conditions. The particle scattering function from a coated cylinder model – see eq. (4) – is calculated as:

$$P(q)=\int_0^{\frac{\pi}{2}}\left|\frac{\Delta\rho_{in}r_{in}^2 2\pi h\cdot G(q,\beta;r_{in})+\Delta\rho_{out}r_{out}^2 2\pi h\cdot G(q,\beta;r_{out})+\Delta\rho_{out}r_{in}^2 2\pi h\cdot G(q,\beta;r_{in})}{(\Delta\rho_{in}-\Delta\rho_{out})r_{in}^2 2\pi h+\Delta\rho_{out}r_{out}^2 2\pi h}\right|^2\times\sin\beta d\beta \quad (4)$$

where $\Delta\rho_{in}$ and $\Delta\rho_{out}$ are the difference of the electron density between solvent and the inner / outer cylinder specified by the radius r_{in} and r_{out}, respectively (see Figure 3). The function G(q, β; x) is defined by equation (5) as:

$$G(q,\beta;x)=\frac{\sin(2\pi Hq\cdot\cos\beta)\cdot 2J_1(qx\sin\beta)}{(2\pi Hq\cdot\cos\beta)(qx\sin\beta)} \quad (5)$$

with H being the cylinder´s half-length and $J_1(S)$ being a first-order Bessel function of the argument S.

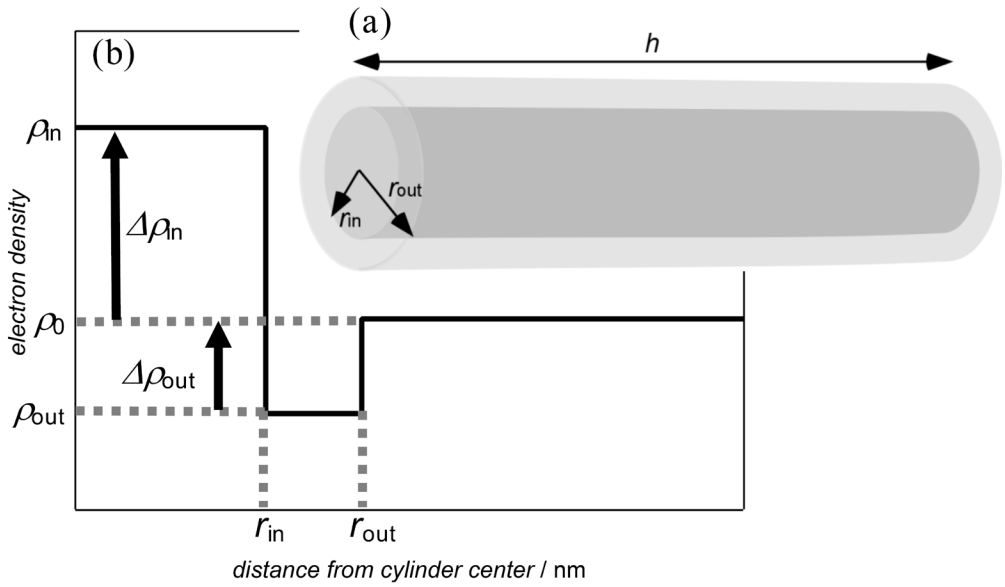

198

199 **Figure 3.** (a) Coaxial double-layer cylinder, (b) schematic electron density profile across the
200 cylinder.

201

202 It is reported that the volumetric mass density of the mixed solvent of EMIm-OAc/water has
203 the highest value around at 15 wt% of water (Cho et al. 2011), indicating that the electron
204 density of solvent will increase with the water content until 15 wt% by the formation of an
205 EMIm-OAc/water complex. EMIm-OAc involved in the solvation of cellulose may have
206 different characteristics from pure bulk IL when the water content increases, because the
207 packing state of EMIm-OAc will be different from that in bulk IL and also the electron density
208 of the solvent will increase with added water. Indeed, MD simulation results suggested that the
209 solvent composition near cellulose is different from the bulk in EMIm-OAc/water/cellulose
210 solution (Le et al. 2014; Ghoshdastider et al. 2016). Accordingly, a cellulose chain in the mixed
211 solvent (EMIm-OAc/water) is surrounded by a layer of dispersedly packed EMIm-OAc, which
212 has a lower electron density when averaged over the sheath (intermediate) layer than the outer
213 solvent. A cellulose chain in EMIm-OAc/water is approximately represented by a coaxial
214 double layer cylinder specified by an inner radius r_{in} and an outer radius r_{out} with the core and
215 sheath being distinguished by the difference in electron density. The model and the variation of
216 electron densities in the radial direction are schematically shown in Figure 3, where the core
217 and sheath are supposed to be constituted of cellulose and solvation shell, respectively.

218

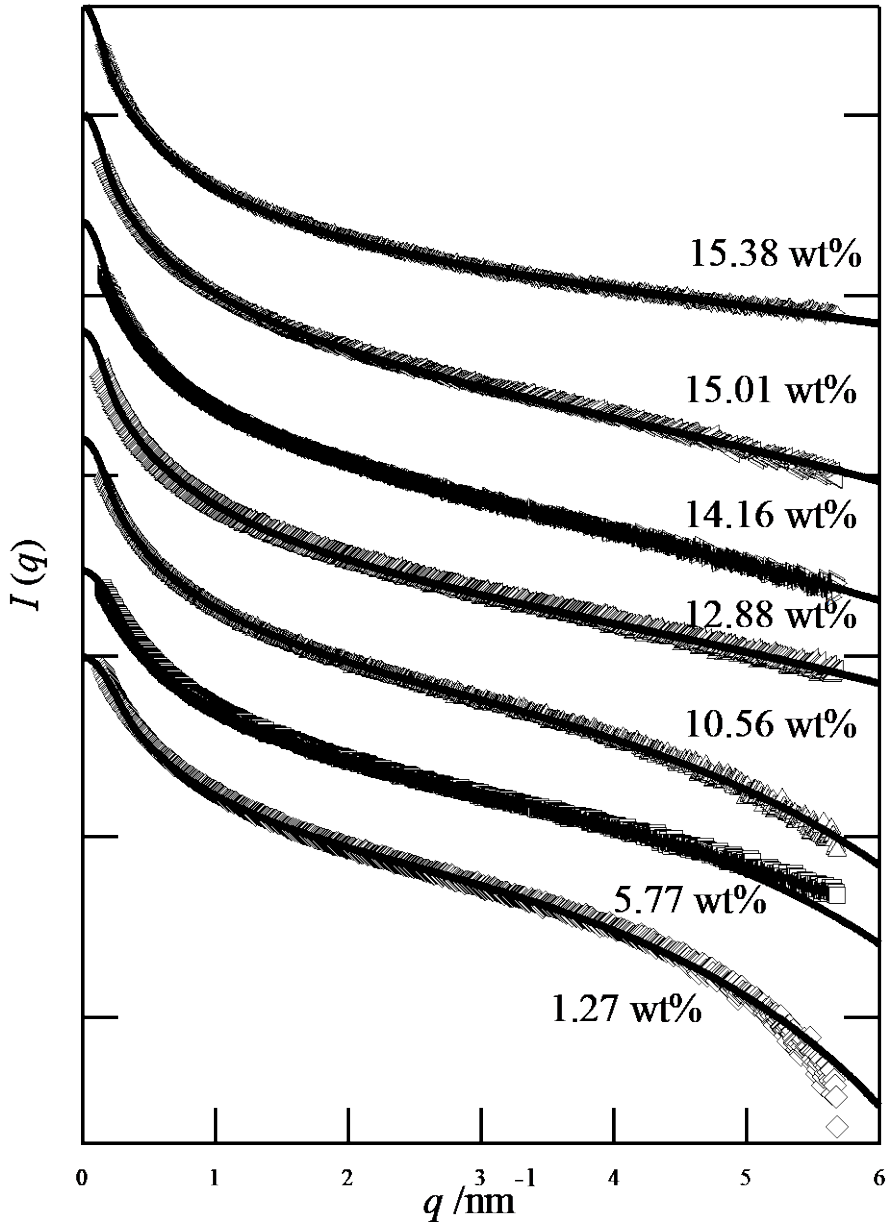

Figure 4. Observed SAXS profiles and simulated profiles with a coaxial double-layer cylinder model for cellulose in the mixed solvent system EMIm-OAc/water (water content indicated).

The observed scattering profile was simulated according to Eq. 4 to optimize the fitting to the observed profiles with three parameters; the inner radius r_{in} and the outer radius r_{out} of the cylinder with a constrain that $\Delta\rho_{in} - \Delta\rho_{out} = 1$. The cylinder length 2H serves as a measure for the range of rod-like characteristics in a long semi-flexible cellulose chain, which is a low impact parameter in the fitting procedure.

Table 1. Calculated parameters of the coaxial double-layer cylinder model by fitting to the experimental SAXS profiles.

content of water in solvent [wt%]	r_{in} [nm]	r_{out} [nm]	r_{out}-r_{in} [nm]	$\Delta\rho_{in}$	$\Delta\rho_{out}$	h [nm]
1.27	0.54	0.95	0.41	0.862	-0.138	5.0
5.77	0.50	0.81	0.31	0.769	-0.231	5.0
10.56	0.49	0.66	0.17	0.633	-0.367	5.0
12.88	0.37	0.50	0.13	0.625	-0.375	6.0
14.16	0.37	0.47	0.10	0.625	-0.375	6.0
15.01	0.37	0.48	0.11	0.571	-0.429	7.0
15.38	0.35	0.48	0.13	0.500	-0.500	7.0

Figure 4 shows the fitting results, demonstrating a superb agreement with the experiment. The parameters used in Eq. 4 are summarized in Table 1. When the water content is lower than 10 wt%, the inner radius of the model cylinder is around 0.50 nm (0.35 nm in terms of the radius of gyration), which is consistent with the cross-sectional radius estimated for a single cellulose chain in the cellulose crystal I. The inner radius drops to 0.37 nm (0.26 nm in terms of the radius of gyration) when the water content exceeds 12 wt%. This value is similar to R_c estimated from molecular dynamics results (Miyamoto et al. 2018) of isolated cellulose chains in water. In this work, the cellulose's dihedral angle O5-C5-C6-O6 indicates the local geometry at C6-OH to be a *gt* conformation (56.5 %), less *gg* (37.8 %) and very little *tg* (5.7 %) conformation. A recent MD simulation analysis indicated that the dihedral angle with respect to C6_OH in EMIm-OAc could be different from that in water or in the crystalline state (Liu et al. 2010; Zhao et al. 2013). The outer radius of the model cylinder decreases from 0.95 nm to 0.50 nm with the water content increasing from 1.27 wt% to 12.88 wt%, and the sheath (the intermediate layer) becomes thinner from 0.4 nm to 0.1 nm when the water content is increased over 10 wt%. Considering its thickness, the sheath (the outer shell) is thus considered to consist of an EMIm-OAc monolayer which will be in equilibrium with surrounding free or water-bound EMIm-OAc in terms of hydrogen bonding. When the water content increases to 10 wt%, most of EMIm-OAc is water-bound and water molecules approach the cellulose chain. The water is bound to EMIm-OAc and is not able to interact directly with a cellulose chain at this stage. The

sheath will get thinner because the water-side of the solvent complex will face directly a cellulose chain. This situation will be more pronounced at higher water contents, as the sheath thickness becomes around 0.1 nm (the order of the size of a water molecule) and the electron density in the sheath decreases. The conformation of cellulose is also influenced by the surrounding water molecules, and cellulose assumes a more extended structure. The conformation of a cellulose chain may change from one similar to its crystal state to one similar to an amorphous state, so that the inner radius of the model cylinder becomes smaller to reach the value estimated from the molecular model of cellulose in water. When water contacts the cellulose and interacts directly with it, the intramolecular hydrogen bonding in cellulose chains is promoted, the conformation is changed, and eventually the cellulose chains will collapse. It should be noted that even at this stage there is no free water present. These conclusions from our experimental data agree with predictions from molecular dynamics simulations (Bengtsson et al. 2017).

The process of the conformational change of cellulose dissolved in the EMIm-OAc/water mixed solvent is summarized as follows: When cellulose dissolves in EMIm-OAc, its conformation will change and it will shrink by breaking intra-molecular hydrogen bonds in the chain axis as shown by the MD simulation (Mori et al. 2012). Cellulose is surrounded by a sheath layer of interacting solvent molecules. The introduction of water generates water complexes with EMIm-OAc. ~~excess water as individual molecular phase emerges only when the water content exceeds 40 wt%. Up to this water content, water molecules are bound to EMIm-OAc but not to each other.~~ Water is consumed by forming the complex with EMIm-OAc while cellulose remains dissolved. EMIm-OAc forms a sheath around the cellulose chains, but the sheath will get thinner upon addition of more water. When most of EMIm-OAc is bound to water and thus less free EMIm-OAc is available, more water (bound to EMIm-OAc) penetrates into the EMIm-OAc shell of cellulose to form a new sheath with lower electron density, and it increasingly interacts with cellulose to promote intramolecular hydrogen bonding and by reducing hydrogen bonds with EMIm-OAc. The cellulose chain will expand slightly. We speculate that the cellulose dissolved in EMIm-OAc may change its conformation not only with respect to C6-OH but also along the main chain according to the MD simulation (Cho et al. 2011), with a new pair of $\varphi-\psi$ torsion angles of cellulose in EMIm-OAc causing the shrinkage of the molecule along the chain axis direction.

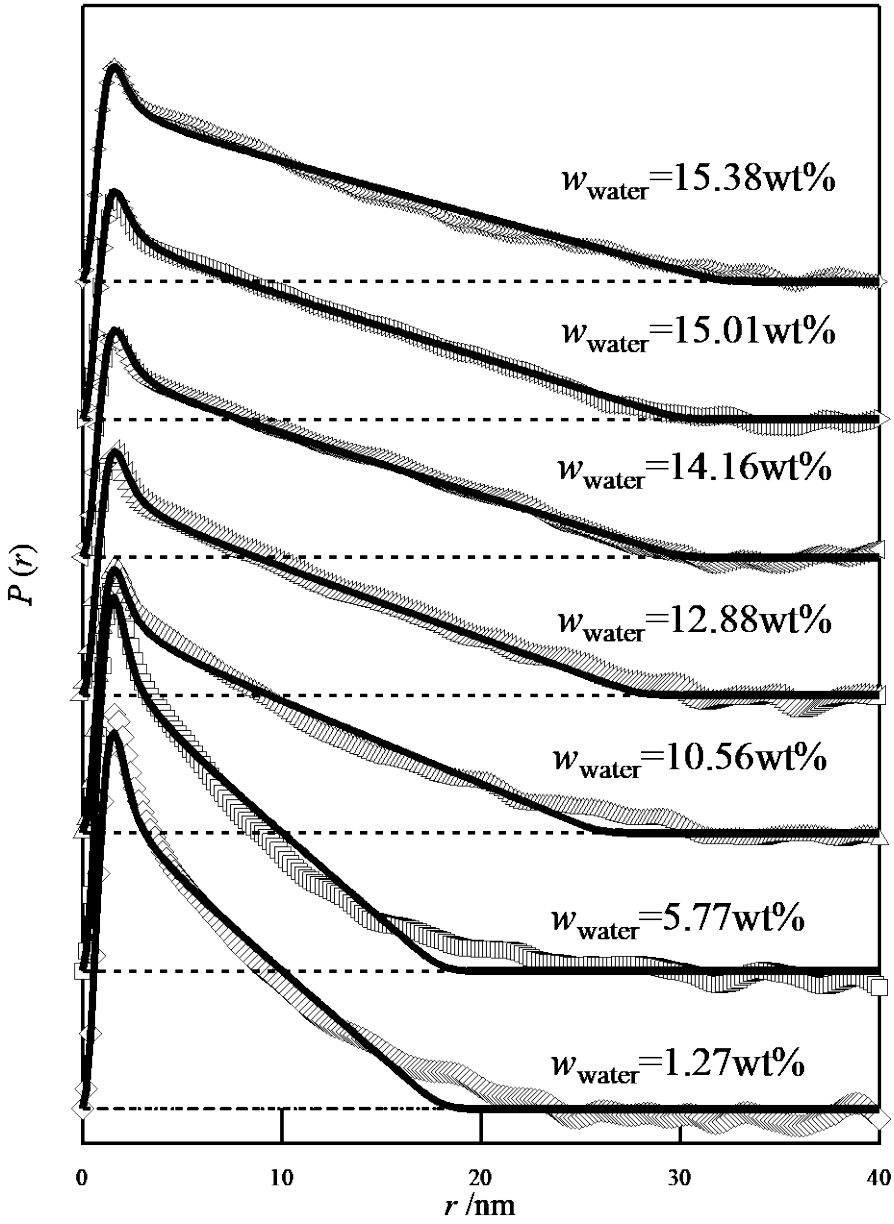

Figure 5. Electronic distance correlation functions obtained from the experimentally observed SAXS profiles and simulated with the corresponding coaxial double-layer cylinder models for cellulose dissolved in EMIm-OAc with various water contents as indicated.

Electronic distance correlation function. The observed SAXS profiles were Fourier-transformed according to eq. (6) into the electronic distance correlation function, P(r) in the real space:

$$P(r) = \frac{1}{2\pi^2}\int_0^\infty I(q)\cdot qr\cdot\sin(qr)\,dq \qquad (6)$$

Similarly, the electronic distance correlation function of the cross section (eq. 7) is calculated as follows:

$$P_c(r) = \frac{1}{2\pi}\int_0^\infty I_c(q)\cdot qr\cdot J_0(qr)\,dq \quad (7)$$

where $J_0(qr)$ is a zero-order Bessel function, and $I_c(q)$ is the scattering intensity from the cross-section.

The electronic distance correlation function represents a pair correlation of a distance between two points in the object in real space. The electronic distance correlation functions obtained from the observed SAXS profiles were compared with those calculated from the corresponding coaxial double layer cylinder models in Figure 5. Although the electronic distance correlation functions obtained from the observed SAXS profiles are smeared by ripples because of the limited range of observation, the corresponding models represent the observed electronic distance correlation functions quite well. The peaks at smaller distances correspond to the distance correlation in radial direction and the linear part at larger distances to the distance correlation in the axial direction. The longer tail at longer distance in the observed function indicates that a cellulose chain is much longer than the range of the fitted cylinder model, and its concave profile is due to the deviation from complete rigidity. When the water content is less than 10 wt%, the simulated cylinder is relatively thick and short. The observed distance correlation function is concave and indicates less rigidity of the cellulose chain. When the water content exceeds 10 wt%, the simulated cylinder becomes thinner and longer. The concave profile increasingly resembles a straight line – thus the rigidity of the cellulose chain has increased, likely due to the onset of the intramolecular hydrogen bonding through the interaction of water. At the onset of cellulose precipitation (water content 10.38 wt%), the observed distance correlation exhibits a complex profile due to the instability of the dissolved state of cellulose. The electronic distance correlation functions confirm the presence of the sheath layer (shell) of a negative electron density. Although some ripples appeared due to the limited range of observation, they did not interfere with the evaluation. The peak position shifts to a shorter distance in accordance with the cross-section getting smaller with increasing water content. Although it might be worthwhile to consider a solvent geometry of concentric cylindrical multilayers (more than one), the present model is not able to analyze such an arrangement.

This situation is better described by means of changes in the electronic distance correlation function of the cross-section (see eq. 7), which was calculated for each cellulose/EMIm-OAc/water solution as shown in Figure 6.

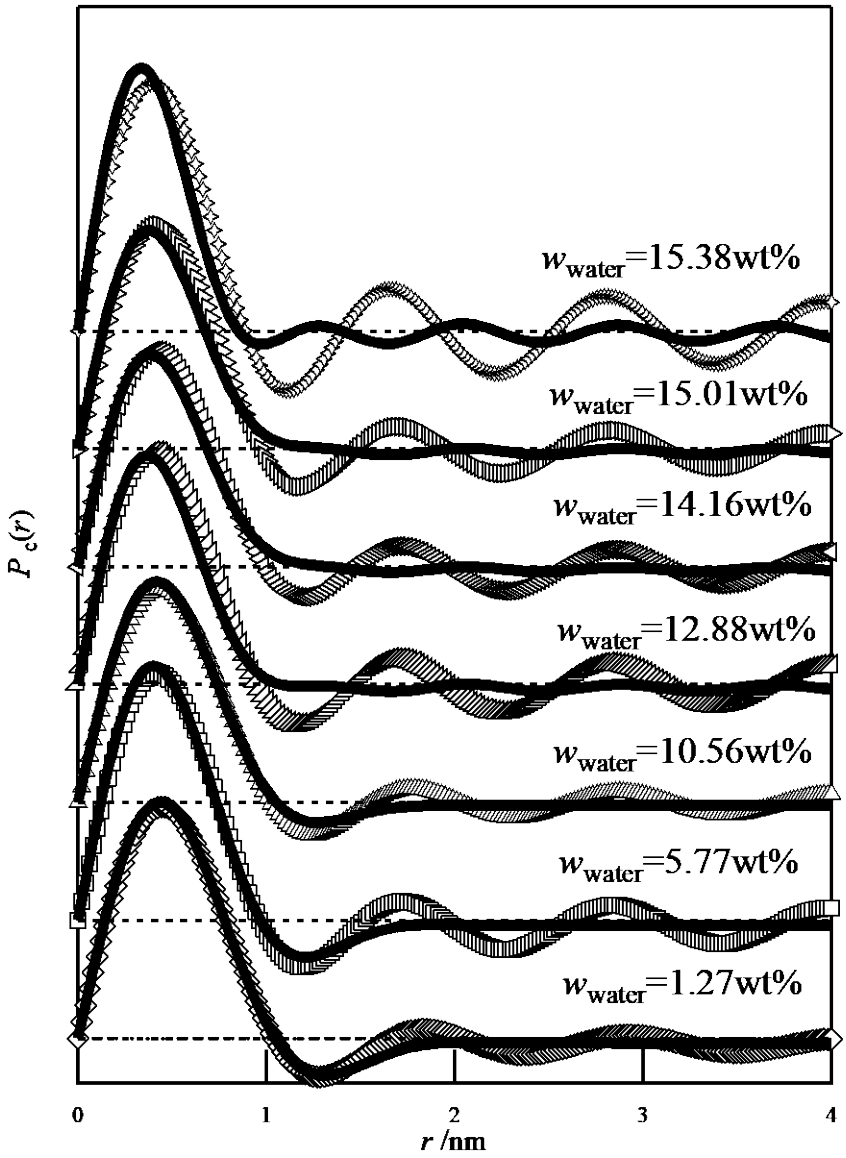

Figure 6. Electronic distance correlation functions for the cross-section obtained from the experimentally observed SAXS profiles and simulated with the corresponding coaxial double-layer cylinder models for cellulose solutions in EMIm-OAc with water contents as indicated.

When the water content was lower than 10 wt%, the electronic distance correlation function for the cross-section exhibited a clear dip (a negative peak) corresponding to the negative electron density in the sheath. The dip position shifts to a shorter distance and the dip depth becomes more shallow with increasing water content, and the dip disappears when the water content exceeds 12 wt%, with the sheath becoming very thin. At the highest water content (15.38 wt%), the electronic distance correlation function for the cross-section became unstable, reflecting the non-equilibrium state of the solution.

Conclusions

We observed with small-angle X-ray scattering the conformational change of cellulose dissolved in an ionic liquid solution (EMIm-OAc) upon adding water. A conventional Guinier approximation for the cross-section of a rigid rod model still holds for the observed SAXS profiles of cellulose in EMIm-OAc/water solution with lower water contents. The apparent cross-sectional radius of gyration R_c was found to decrease with increasing water content in the solvent. However, the Guinier approximation eventually failed to yield a physically reasonable cross-sectional radius of gyration when the water content approached 15 wt%, near the cellulose precipitation limit.

A coaxial double-layer cylinder model was adapted to explain these singular characteristics of the change of scattering profiles and the physically meaningless (negative) apparent cross-sectional radius of gyration according to the conventional Guinier approximation for a cross-section of a rod-like molecule. The model comprises a sheath (an outer shell) and a core, which represents the cellulose chain surrounded by the sheath-forming solvent. The core and the sheath are characterized by different electron densities, and the sheath is virtually formed by the interaction of a cellulose chain with EMIm-OAc. Since the interaction sites along the cellulose chains are limited and the size of EMIm-OAc is relatively large, EMIm-OAc molecules align along a cellulose chain sparsely and the electronic density of the sheath becomes lower than in the bulk solvent phase. When water is added, EMIm-OAc is hydrated and the electron density of the solvent (complexes) increases further. When most of EMIm-OAc molecules are hydrated upon further water addition, water sites get increasingly in contact with the cellulose chain and influence the cellulose chain´s conformation. The sheath (outer shell) becomes apparently thinner, and the electron density of the sheath further decreases. The interaction with water promotes the intramolecular hydrogen bonding in a cellulose chain, although the interaction of water with a cellulose chain is not yet so strong at first to cause precipitation, and complex formation with EMIm-OAc is still operative. This agrees with previous MD simulations that suggested that the backbone of cellulose chain in IL is more flexible than in water. The present analysis in terms of a coaxial double-layer cylinder model clearly indicates that the cellulose chain changes its conformation and becomes stiffer by intramolecular hydrogen bonding through the interaction with water. When the water content exceeds 15 wt %, the sheath cannot be formed.

An important conclusion from the present analysis is also that the conventional way to evaluate an excess scattering by a simple subtraction of solvent scattering from solution scattering may fail in some cases. Enough care should be taken to analyze the electromagnetic wave scattering

especially in the case of the mixed solvents in which a preferential solvation might take place leading to layers of different electron densities surrounding solute molecules.

Acknowledgements

This work was performed under the approval of the Photon Factory Program Advisory Committee (Proposal No. 2014G604 and 2015G147). This work was financially supported by the Center for Fiber Textile Science in Kyoto Institute of Technology, and the Astrian Biorefinery Center Tulln (ABCT). We gratefully acknowledge and the work of past and present members of our laboratories involved in the work.

References

Ahn K, Zaccaron S, Rosenau T, Potthast A (2019) How alkaline solvents in viscosity measurements affect data for oxidatively damaged celluloses. Part 1. Cupri-ethylenediamine (CED, cuen). Biomacromol. 20(11):4117-4125.

Barthel S, Heinze T (2006) Acylation and carbanilation of cellulose in ionic liquids. Green Chem. 8:301-306.

Bengtsson J, Olsson C, Hedlund A, Köhnke T, Bialik E (2017). "Understanding the Inhibiting Effect of Small-Molecule Hydrogen Bond Donors on the Solubility of Cellulose in Tetrabutylammonium Acetate/DMSO." J. Phys. Chem. B 121(50): 11241-11248.

Chen Y, Zhang Y, Ke F, Zhou J, Wang H, Liang D (2011) Solubility of neutral and charged polymers in ionic liquids studied by laser light scattering. Polymer 52:481-488.

Cho H M, Gross A S, Chu J W (2011) Dissecting force interactions in cellulose deconstruction reveals the required solvent versatility for overcoming biomass recalcitrance. J. Am. Chem. Soc. 133:14033-14041.

Ebner G, Schiehser S, Potthast A, Rosenau T (2008) Side reaction of cellulose with common 1-alkyl-3-methylimidazolium-based ionic liquids.4. Tetrahedron Lett. 49:7322-732.

Fendt S, Padmanabhan S, Blanch H W, Prausnitz J M (2011) Viscosities of Acetate or Chloride-

Based Ionic Liquids and Some of Their Mixtures with Water or Other Common Solvents. J. Chem. Eng. Data 56:31-34.

Fukaya Y, Hayashi K, Wada M, Ohno H (2008) Cellulose dissolution with polar ionic liquids under mild conditions: required factors for anions. Green Chem. 10:44-46.

Gericke M, Schlufter K, Liebert T, Heinze T, Budtova T (2009) Rheological properties of cellulose / ionic liquid solutions: from dilute to concentrated states. Biomacromol. 10:1188-1194.

Ghoshdastidar D, Senapati S (2016) Ion-water wires in imidazolium-based ionic liquid/water solutions induce unique trends in density. Soft Matter 12:3032-3045.

Heinze T, Schwikal K, Barthel S (2005) Ionic liquids as reaction medium in cellulose functionalization. Macromol. Biosci. 5:520-525.

Hedlund A, Köhnke T., Theliander H (2015) Coagulation of EmimAc-cellulose solutions: dissolution-precipitation disparity and effects of non-solvents and cosolvent. Nordic pulp paper Res. J. 30(1):32-42.

Henniges U, Kostic M, Borgards A, Rosenau T, Potthast A (2011) Dissolution Behavior of Different Celluloses. Biomacromol. 12:871-879.

Kajiwara K, Wataoka I (2016) The Method of Small-Angle X-ray Scattering and Its Application to the Structural Analysis of Oligo- and Polysaccharides in Solution. In: Matricardi P, Alhaique F, Coviello T (eds) Polysaccharide Hydrogels: Characterization and Biomedical Applications. Pan Stanford Publishing, Singapore, pp 265-323.

Koide M, Wataoka I, Urakawa U, Kajiwara K, Henniges U, Rosenau T (2019) Intrinsic Characteristics of Cellulose Chain in Ionic Liquid: the Shape of a Single Cellulose Molecule. Cellulose 26(4):2233-2242.

Le K A, Sescousse R, Budtova T (2011) Influence of water on cellulose-EMIm-OAc solution properties: a viscometric study. Cellulose 19:45-54.

Le K A, Rudaz C, Budtova T (2014) Phase diagram, solubility limit and hydrodynamic properties of cellulose in binary solvents with ionic liquid. Carbohydr. Polym. 105:237-243.

Liu H, Sale KL, Holmes BM, Simmons BA, Singh S (2010) Understanding the Interactions of Cellulose with Ionic Liquids: A Molecular Dynamics Study. J. Phys. Chem. B 114:4293-4301.

Liebner F, Ebner G, Becker E, Potthast A, Rosenau T (2010) Thermal aging of 1-alkyl-3-methylimidazolium ionic liquids and its effect on dissolved cellulose. Holzforschung 64:161-166.

Livsey I (1987) Neutron Scattering from Concentric Cylinders. J. Chem. Soc., Faraday Trans. 2 83:1445-1452.

Lynden-Bell R M, Del Popolo M G, Youngs T G, Kohanoff J, Hanke C G, Harper J B, Pinilla C C (2007) Simulations of ionic liquids, solutions, and surfaces. Acc. Chem. Res. 40:1138-1145.

Mazza M, Catana DA, Vaca-Garcia C, Cecutti C (2008) Influence of water on the dissolution of cellulose in selected ionic liquids. Cellulose 16: 207-215.

Miyamoto H, Sakakibara K, Wataoka I, Tsujii Y, Yamane C, Kajiwara K (2018) Interaction of Water Molecules with Carboxyalkyl Cellulose. In: Potthast A, Rosenau T (eds.) Advances in Cellulose Science and Technology: Chemistry, Analysis, and Applications. Wiley, pp 127-141.

Mori T, Chikayama E, Tsuboi Y, Ishida N, Shisa N, Noritake Y, Moriya S, Kikuchi J (2012) Exploring the conformational space of amorphous cellulose using NMR chemical shifts. Carbohydr. Polym. 90:1197-1203.

Moulthrop J S, Swatloski R P, Moyna G, Rogers R D (2005) High-resolution ^{13}C NMR studies of cellulose and cellulose oligomers in ionic liquid solutions. Chem. Commun. 12:1557-1559.

Olsson C, Idstrom A, Nordstierna L, Westman G (2014) Influence of water on swelling and dissolution of cellulose in 1-ethyl-3-methylimidazolium acetate. Carbohydr. Polym. 99:438-

446.

Parviainen H, Parviainen A, Virtanen T, Kilpelainen I, Ahvenainen P, Serimaa R, Gronqvist S, Maloney T, Maunu S L (2014) Dissolution enthalpies of cellulose in ionic liquids. Carbohydr. Polym. 113:67-76.

Potthast A, Rosenau T, Henniges U, Schiehser S, Kosma P, Saake B, Lebioda S, Radosta S, Vorwerg W, Wetzel H, Koschella A, Heinze T, Strobin G, Sixta H, Strlic M, Isogai A. (2015) Comparison testing of methods for gel permeation chromatography of cellulose: Coming closer to a standard protocol. Cellulose 22(3):1591 – 1613.

Rabideau BD, Agarwal A, Ismail AE (2013) Observed mechanism for the breakup of small bundles of cellulose I(alpha) and I(beta) in ionic liquids from molecular dynamics simulations. J. Phys. Chem. B 117:3469-3479.

Rosenau T, Potthast A, Kosma P, Chen C L, Gratzl J S (1999) Autocatalytic Decomposition of *N*-Methylmorpholine-*N*-oxide Induced by *Mannich* Intermediates. J. Org. Chem. 64:2166-2167.

Rosenau T, Potthast A, Kosma P, Saariaho AM, Vuorinen T, Sixta H (2005) On the nature of carbonyl groups in cellulosic pulps. Cellulose 12:43-50.

Swatloski R P, Spear S K, Holbrey J D, Rogers R D (2002) Dissolution of Cellulose with Ionic Liquids. J. Am. Chem. Soc. 124:4974-4975.

Uto T, Yamamoto K, Kadokawa J (2018) Cellulose Crystal Dissolution in Imidazolium-Based Ionic Liquids: A Theoretical Study. J. Phys. Chem. B 122:258-266.

Youngs T G A, Holbrey J D, Mullan C L, Norman S E, Lagunas M C, D'Agostino C, Mantle M D, Gladden L F, Bowron D T, Hardacre C (2011) Neutron diffraction, NMR and molecular dynamics study of glucose dissolved in the ionic liquid 1-ethyl-3-methylimidazolium acetate. Chem. Sci. 2:1594-1605.

Zhao Y, Liu X, Wang J, Zhang S (2013) Effects of anionic structure on the dissolution of cellulose in ionic liquids revealed by molecular simulation. Carbohydr. Polym. 94:723-730.